

University of Windsor
Scholarship at UWindsor

Physics Publications

Department of Physics

4-2010

Metastable oxygen atom detection using rare gas matrices

Wladyslaw Kedzierski
University of Windsor

E Blejdea
University of Windsor

Aldo DiCarlo

J. W. Mcconkey
University of Windsor

Follow this and additional works at: <https://scholar.uwindsor.ca/physicspub>

 Part of the [Physics Commons](#)

Recommended Citation

Kedzierski, Wladyslaw; Blejdea, E; DiCarlo, Aldo; and Mcconkey, J. W.. (2010). Metastable oxygen atom detection using rare gas matrices. *Journal of Physics B: Atomic, Molecular and Optical Physics*, 43 (8). <https://scholar.uwindsor.ca/physicspub/190>

This Article is brought to you for free and open access by the Department of Physics at Scholarship at UWindsor. It has been accepted for inclusion in Physics Publications by an authorized administrator of Scholarship at UWindsor. For more information, please contact scholarship@uwindsor.ca.

Metastable oxygen atom detection using rare gas matrices

W Kedzierski, E Blejdea, A DiCarlo and J W McConkey

Physics Department, University of Windsor, Ontario N9B 3P4, Canada.

Abstract: The use of solid rare gas matrices as detectors of metastable oxygen atoms is investigated. A 100 eV electron beam colliding with N₂O target gas is used as the source of O(¹S). Parameters considered are surface temperature, time delay of excimer emission and spectral response to O(¹S). In all cases detector sensitivity maximised at temperatures $\leq 20\text{K}$. Krypton was found to provide the most sensitive surface and Ne the least.

PACS #: 34.80 Dp and Ht, 33.20 kf, 37.20 +j, 34.35 +a

Introduction

Metastable atomic species play important, sometimes dominant roles in a variety of situations ranging from planetary atmospheres to low temperature plasmas and biological environments [see e.g. Rees (1989), Rochkind and Ouaknine (1992), McConkey et al (2008)]. Oxygen metastable species, O(¹S), O(¹D) and O(⁵S), are of particular interest as far as earth's atmosphere is concerned.

Because of their long lifetimes, single particle detection of most metastable species is very difficult in the laboratory. Various attempts to detect oxygen metastable such as using Auger emission from a low work function surface [Gilpin and Welge (1971), Alcock and McConkey (1978)], using a chemi-ionization process [Stone et al (1976)], or by detection of inelastically scattered electrons, all suffered from a lack of discrimination against other atomic or molecular species in addition to not being particularly sensitive.

More recently laser or synchrotron based techniques such as REMPI or VUV Ionization have been used to monitor production of specific fragments [e.g. Kimmel and Orlando (1995), Lu et al (2003)].

In the case of O(¹S) LeClair and McConkey (1993) solved the problems of both sensitivity and selectivity by using a solid Xe surface at 65K as the basic detector element. The O(¹S) atoms which reached this surface formed XeO excimers which promptly radiated. The wavelength of the emission was red shifted from the original green auroral line feature at 557.7 nm. Using this single particle detector we have been able to study quantitatively the dissociation channels of a large number of oxygen-containing molecules where the O(¹S) fragment results [see McConkey et al (2008)]. We demonstrated also that the Xe matrix acts as an efficient detector for S(¹S) [Kedzierski et al, (2001)] and for CO(^a3Π) [LeClair and McConkey (1994), LeClair et al (1994)]. In the present set-up we used a plexiglass light pipe between the cold finger and the photomultiplier to enhance the detection efficiency in the visible and near infrared regions and, since this does not transmit in the UV, we currently can not study the CO* excimers which radiate at 325 nm [see LeClair et al (1994)] and which might be produced from targets such as CO or CO₂.

The concept of using excimer formation in a solid rare gas matrix to shorten the lifetimes of metastable atoms goes back to earlier work where small quantities of oxygen containing molecules were frozen out in solid deposits of rare gases and then bombarded with electrons or energetic photons [Taylor et al (1981), Walker et al (1981), Schoen and Broida (1960), Lawrence and Apkarian (1992), Maillard et al, (1985), Girardet et al (1986), Goodman et al (1977), Belov and Yurtaeva (2001)]. The mechanisms which governed the processes involved were well studied and understood. Ne, Ar and Kr matrices were observed to give outputs similar to Xe though with individual spectral signatures.

In an attempt to probe further the usefulness of the rare gas matrices as detectors of metastable atoms, particularly oxygen, we have extended our work to lower temperatures so that matrices other than Xe could be studied. We have studied the responses of the matrices as a function of temperature and have established the spectral variation of the outputs from each rare gas. The current study is limited to a study of the detection capabilities of the various matrices for O(¹S). Future work will consider how the different surfaces respond to other metastable species such as S(¹S).

Experimental Techniques:

A block diagram of the current apparatus is shown in figure 1. Turbomolecular pumps provided a base pressure in the main chamber of less than 10⁻⁶ Torr. Typically this rose to 1.5-2 x 10⁻⁶ Torr when the target gas beam was introduced. A pulsed electron beam from a magnetically confined gun impacts the target gas beam and the resulting fragments drift to the detector which is placed in a separate chamber. A low pressure rare gas is continuously frozen out on the cryogenically cooled finger so that a rare gas matrix layer is formed. Prior to introducing the rare gas, the base pressure in the cold finger chamber was

less than in the main target chamber because of the additional cryopumping which occurred in that region. The rare gas was leaked into the cold finger chamber continuously, as previous work [LeClair and McConkey, 1993] had demonstrated increased sensitivity was achieved by continuously refreshing the surface of the film. The leak rate was chosen to optimize the detector sensitivity and was kept an order of magnitude lower than the rate where in-flight collisional deactivation of the metastable atoms, en route to the cold finger surface, was clearly contributing.

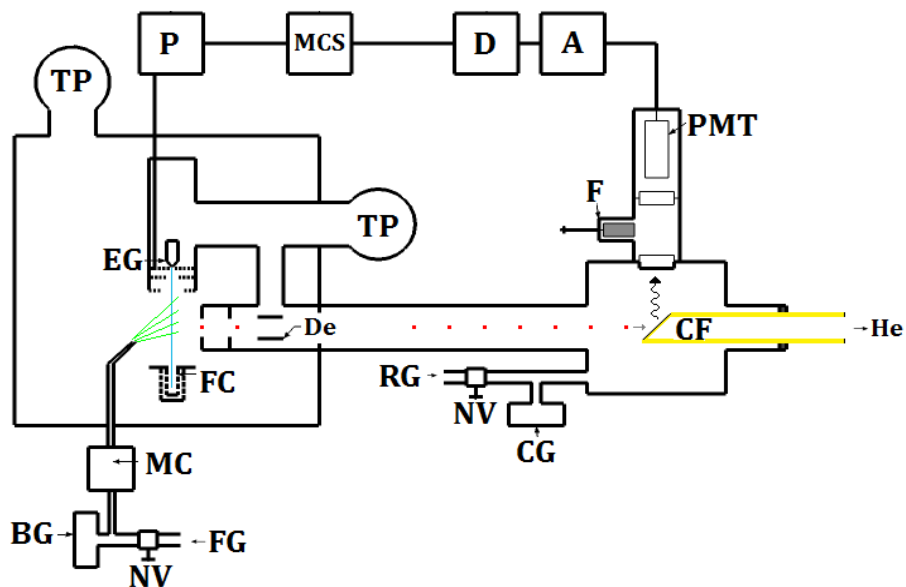


Figure 1. Block diagram of the metastable atom detector system. A, amplifier; D, discriminator; P, pulser; F, filter; TP, turbopump; EG, electron gun; FC, Faraday cup; MC, microwave cavity; BG, Baratron gauge; NV, needle valve; CG, convection gauge; CF, cold finger; He, helium cryostat; RG, rare gas; De, deflector plates; FG, feed gas; MCS, multichannel scaler; PMT, photomultiplier tube.

The temperature of the cooled finger is controlled by an Advanced Research Systems, Inc. DE-202 cryogenic unit. Oxygen metastables incident on the cold surface thermalise, form excimers and radiate. The resultant photons are detected by the R943-02 HAMAMATSU photomultiplier, cooled to -30°C , and the pulses are routed to a multichannel scaler (MCS). The manufacturer's data sheet indicated a smooth drop off in quantum efficiency from about 17 to 13 % over the wavelength range (500-750 nm) of interest in the present work. The zero of the timescale on the MCS is established by the prompt photons which result from excitation of the target particles during the e-beam pulse and their subsequent scattering into the photomultiplier from the cold finger. For all the work reported here an e-beam pulse width of $10\ \mu\text{s}$ was used. The width of the prompt photon signal is identical to this as can be seen from Figure 2. The shape of this prompt photon signal did not depend on which rare gas matrix was being used but its magnitude depended on parameters such as film thickness and transmission. We did not investigate these effects quantitatively.

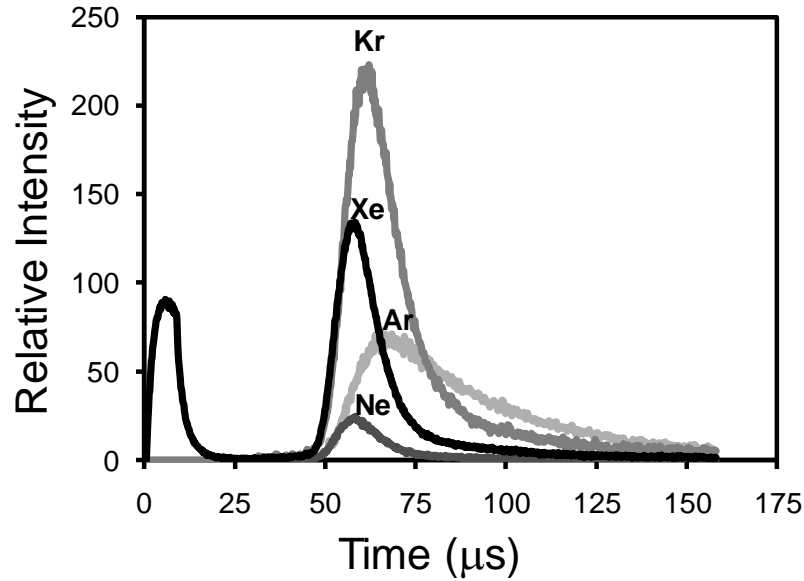


Figure 2. O(1S0) TOF data for different rare gas matrices. Note that the data for the different matrices have not been normalized to one another. The individual data sets have been scaled so that differences are clearly visible. The e-beam energy was 100 eV in each case and the target was N₂O. The e-beam pulse width was 10 μs in each case. The cold finger temperature was 20K in each case. Note that the prompt photon peak starting at time zero has been suppressed for all the matrices except Xe for reasons of clarity.

Figure 2 shows a sample of the time-of-flight (TOF) data obtained at an e-beam energy of 100 eV. N₂O is chosen as the target gas because it had been shown earlier [LeClair and McConkey (1993)] that a single dissociation channel dominated O(¹S) production and also that no other metastable or Rydberg fragments from this target affected the detector when Xe was used. The data have not been normalized relative to one another. First of all, the figure illustrates that all four of the rare gas matrices, neon, argon, krypton and xenon, show sensitivity to the impacting O(¹S) atoms. Note that the prompt photon peak has been suppressed for clarity for all the detector surfaces except xenon. We note also that the basic shape of the TOF peak is the same for all surfaces except that a noticeable shift is evident in the case of argon. The lifetime of O(¹S) in the gas phase is much too long (0.74 μs) for in flight decay to be responsible. A more likely scenario is that, with Ar, the excimer lifetime appears to be more than 20 microseconds. There is the possibility of small shifts for the other targets as well. We have modeled the situation by introducing an exponential factor, exp[-t/τ], where τ represents the excimer lifetime. The modeling was based on the following equation:

$$f(t) = \int_{-\infty}^t f_{Xe}(t') \cdot \exp(-(t - t')/\tau) \cdot dt'$$

Where $f(t)$ defines the time evolution of the detected signal when a rare gas other than Xe is used, and $f_{Xe}(t')$ is the time evolution of the detected signal from the XeO excimer. We have found the lifetimes for Ne, Kr and Ar, which provide the best fit to the data, to be 0.2, 4.2 and 23.4 μs respectively. The

lifetime of the XeO excimer is known to be about 200 ns [Lawrence and Apkarian (1992)] and thus is insignificant on the timescale of figure 2.

It is possible to make some comparisons between these lifetimes and those obtained from studies where rare gas matrices with small admixtures of oxygen-containing species were formed and then bombarded by either energetic electrons or photons. Thus Monaghan and Rehn (1978), using a 1% N₂O contaminant in Kr at a temperature of 25 K and bombarding with 9.5 eV photons from a pulsed synchrotron source, found KrO* lifetimes of 1.4 and 3.6 μs. The two lifetimes corresponded to transitions of slightly different energies (wavelengths) in the matrix. Danilychev and Apkarian (1993) quote lifetimes of 1.4 and 11 μs for the same KrO* emissions. They assign the two different transitions to O atoms isolated in different (interstitial and substitutional) lattice sites in the matrix Taylor et al(1981) measured lifetimes of KrO* ranging from 0.5 to 1.5 μs when using 1% CO₂ in a Kr matrix and bombarding with 11.05 eV photons. They found that the lifetime was affected by the temperature of the matrix. Taylor et al (1981) quote lifetime values of 40 and 20 μs for the ArO* emissions from an Ar matrix with 1% N₂O content and 11 eV photon bombardment. The latter lifetime is in reasonable agreement with the 24μs obtained in the present work. Since the measured lifetime seems to be a function of the wavelength of the RgO* emission being considered, some further discussion of the spectral distribution of the rare gas-oxygen excimer radiation is given in a later section.

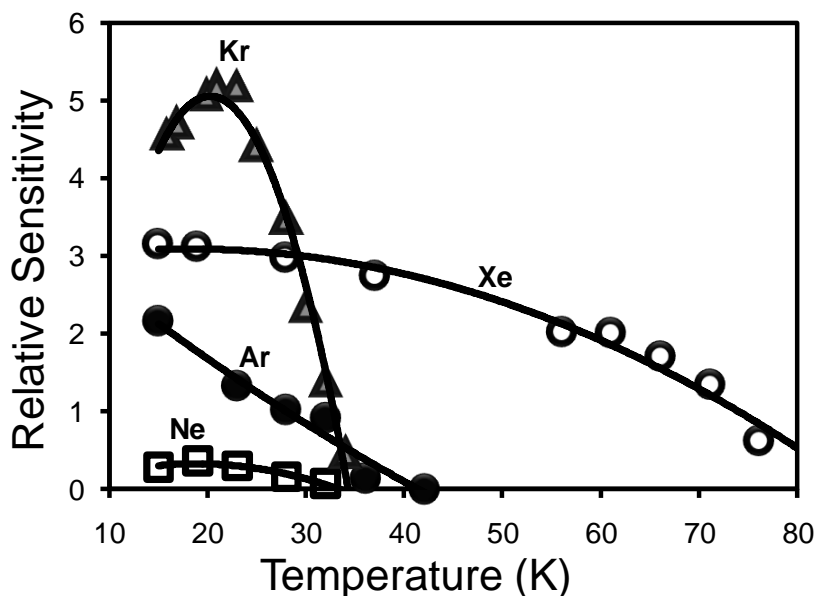


Figure 3. Variation of the sensitivity of the different matrices with cold finger temperature. Triangles, Kr; squares, Xe; circles, Ar; diamonds, Ne. Lines have been drawn through the experimental points to help guide the eye. Data are the average of a number of runs in each case and have been corrected for any variations in current and source pressure as well as for variations in the PMT quantum efficiency and length of data taking run. See text for further details.

Figure 3 shows how the sensitivities of the different surfaces vary with the surface temperature. Here again N₂O has been used as the target gas and the incident e-beam energy is 100 eV. For Xe this represents an extension of earlier work by Kedzierski et al (1998) where data were limited to temperatures above 63K. Note that the data have been corrected for variations in O(¹S) production parameters, such as

electron beam current, target gas pressure and length of data taking period, and for variations in the spectral sensitivity of the photon detection system. We note that no filters were used when accumulating the data of Fig 3 and thus the relative photon detection efficiency was obtained directly from the quantum efficiency data provided by the manufacturer. Also, because no filters were used the integrated band radiation (see Figure 4) contributed to the observed signals. In all cases integration between 50 and 100 μ s of the TOF curves was used. [Correct ???]. Figure 3 provides an estimate of the relative sensitivity of the different matrix surfaces. We note that in all cases the sensitivities rise as the cold finger temperature is reduced but tend to plateau (or even drop off slightly) at the lowest temperatures (<20K). It was noticed also that the sensitivity tended to drop off after prolonged data taking periods. This is consistent with the thickening of the rare gas matrix on the cold finger which occurred as time progressed. As thickening occurs a rise in surface temperature results accompanied by a drop in sensitivity.

Work with RgO* emissions from rare gas matrices with small (~ 1%) content of an oxygen containing molecule and excitation with electron or photon bombardment reveals that the emissions were significantly affected by the temperature of the matrices [see e.g. Taylor et al (1981), Fugol et al (1986), Gudipati (1996), Danilychev and Apkarian (1993), Belov et al (2000)]. Fugol' et al (1986) find a rapid drop in luminescence from their samples at temperatures above some critical temperature, somewhat similar to what we observe. They found critical temperatures of ~30K, ~30K and ~17K for Xe, Kr and Ar matrices respectively. They suggest that the phenomenon is related to the mobility of excitons within the crystal. Part of the rise in sensitivity which we observe as the temperature is reduced may be due to the reduction in background pressure in the cold finger chamber which occurs as the temperature of the cold finger is reduced. This reduction in background pressure reduces the possibility of collisional destruction of O(¹S) en route to the detector surface. Unfortunately we were not able to quantify this or to study if and how the surface matrix varied as the temperature was changed. Visual inspection revealed distinct differences in the surface layers of the different rare gases on the cold finger. For example, neon and argon layers were clear and invisible to the naked eye whereas xenon layers at 65K were clearly visible as a white snow-like deposit.

To monitor the spectral content of the emissions from the different surfaces we used a model MC1-03 monochromator by PTR Optical Corporation instead of a filter in the optical path between the cold finger and the photomultiplier (see figure 1). TOF data were accumulated at each wavelength setting of the monochromator at constant electron beam current and energy (100 eV) and constant target N₂O pressure and for a fixed data accumulation time. The integrated metastable count was then plotted as a function of wavelength, Figure 4. We note that, for reasons of low signal intensities when using the monochromator and the consequent necessity to use the broadest possible slits, our wavelength scans were relatively low resolution ones. In figure 4 the peak heights of the resultant spectral curves were normalized to the same value. It was found that the data could be fitted very well by Gaussian curves. For clarity only the data points from Xenon are included in figure 4. The widths of the Ne and Ar curves were similar while the Kr curve was slightly broader and the Xe curve was broader still and very similar to that given by LeClair and McConkey (1993).

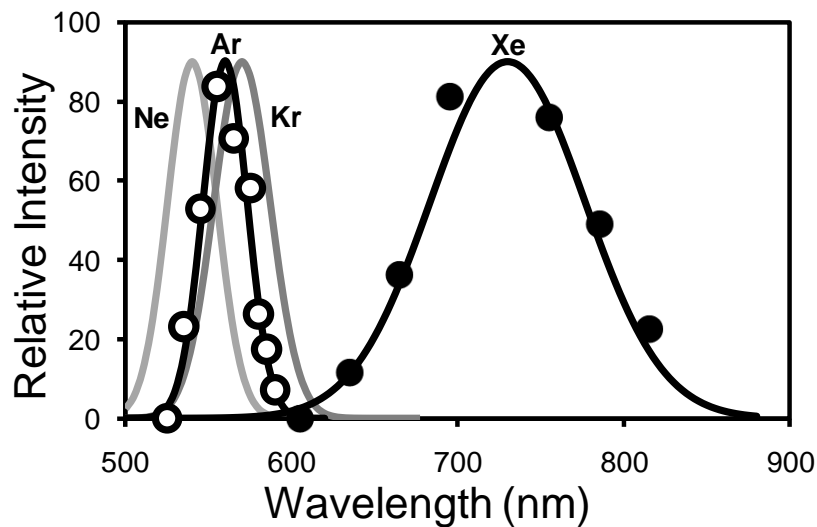


Figure 4. Spectral output from the rare gas matrices as a function of wavelength. Target gas was N_2O in each case and the e-beam energy was 100 eV. Solid lines (Gaussian curves) have been drawn through the experimental points which, except for the case of Xe, have been removed for the sake of clarity. All curves have been normalized to the same peak height. The data for the individual matrices are designated by the rare gas symbols at the peak of each curve. **The temperature of the cold finger was 20K in each case**

We note that the spectral output from the three lighter rare gas matrices are quite close to the atomic $[O(^1S) - O(^1D)]$ transition at 557.7 nm. For Xe the peak in the emission is much broader and occurs at 730 nm. **Good agreement, both in shape and peak position, is obtained with the earlier Xe work of LeClair and McConkey (1993). The different spectral output curves reflect the different excimer potential energy curves for the different rare gases.** We note the remarkably good correlation which exists between the data of figure 4 and the work, noted earlier, where electron or photon bombardment of matrices containing a trace of oxygen occurred [see Taylor et al (1981), Walker et al (1981), Schoen and Broida (1960)].

It is possible, from the parallel work studying the spectral output from RgO^* in doped rare gas crystals, that at higher resolution than was possible in the present work, the spectral output is actually structured with two bands contributing to the single features shown in Figure 4. The mean energies of these bands were 2.22 and 2.28 eV for ArO^* [Taylor et al (1981)], 2.07 and 2.18 eV for KrO^* [Monaghan and Rehn (1978), Taylor et al (1981)] and 1.8 and 1.72 eV for XeO^* [Belov and Yurtaeva (2001)]. The relative magnitude of the two peaks was a function of the temperature of the matrix and its history of annealing. For this reason, and because we are dealing with atoms impinging on the surface of the matrix rather than originating within the material, it is difficult to make any direct comparison between the two situations.

Conclusions

Use of solid rare gas matrices as detectors for metastable O(¹S) atoms has been studied and their behavior quantified as a function of surface temperature. The spectral output from the different matrices has been established. **Effective** lifetimes of the NeO*, KrO* and XeO* excimers are short (4.2μs or less) but for ArO* the **effective** lifetime is much longer (23.4μs). The current work should allow design and development of an optimum detector for O(¹S), for example in a planetary atmosphere environment. Based on previous work, [Kedzierski et al, (2001)], we anticipate that these surfaces should also be sensitive detectors of S(¹S) and possibly of other metastable species as well.

Acknowledgements:

The authors are grateful to the Canadian Natural Sciences and Engineering Research Council (NSERC), to the Canadian Foundation for Innovation (CFI), and to the Ontario Innovation Fund, (OIF), for financial support for this work. The skilled assistance of the Physics electronic and mechanical workshop staff at the University of Windsor is gratefully acknowledged also.

References:

- G. Allcock and J. W. McConkey, *Chem. Phys.* 34, 169 (1978).
A G Belov and E M Yurtaeva, *Fizika Nizkikh Temperatur*, 27, 1268, (2001). *Eng Trans: Low Temp Phys*, 27, 938, (2001).
A G Belov, I Ya Fugol, E M Yurtaeva and O V Bazhan, *J Luminesc*, 91, 107, (2000).
A V Danilychev and V A Apkarian, *J Chem Phys*, 99, 8617, (1993).
I Ya Fugol', A G Belov and E I Tarasova, *JETP Letts*, 43, 687, (1986).
R. Gilpin and K. H. Welge, *J. Chem. Phys.* 55, 975 (1971).
C Girardet, D Maillard and J Fournier, *J Chem Phys*, 84, 4429, (1986).
J Goodman, J C Tully, V E Bondybey and L E Brus, *J Chem Phys*, 66, 4802, (1977).
M S Gudipati, *Chem Phys Letts*, 248, 452, (1996).
W Kedzierski, J Derbyshire, C Malone and J W McConkey, *J Phys B*, 31, 5361, (1998).
W Kedzierski, J Borbely and J W McConkey, *J Phys B*, 34, 4027, (2001).
G A Kimmel and T M Orlando, *Phys Rev Lett*, 75, 2606, (1995).
W G Lawrence and V A Apkarian, *J Chem Phys*, 97, 2229, (1992).
L R LeClair and J W McConkey, *J Chem Phys*, 99, 4566, (1993).
L R LeClair and J W McConkey, *J Phys B*, 27, 4039, (1994).
L R LeClair, M D Brown and J W McConkey, *Chem Phys*, 189, 769, (1994).
I-C Lu, J J Lin, S-H Lee, Y T Lee and X Yang, *Chem Phys Lett*, 382, 665, (2003).
D Maillard, J Fournier, H H Mohammed and C Girardet, *J Chem Phys*, 78, 5480, (1983).
J W McConkey, C P Malone, P V Johnson, C Winstead, V McKoy and I Kanik, *Phys Repts*, 466, 1, (2008).
M. H. Rees, "Physics and Chemistry of the Upper Atmosphere", (Cambridge University Press, Cambridge, 1989).
S Rochkind and G E Ouaknine, *Neurol Res*, 14, 2, (1992).
L J Schoen and H P Broida, *J Chem Phys*, 32, 1184, (1960).
E. J. Stone, G. M. Lawrence, and C. E. Fairchild, *J. Chem. Phys.* 65, 5083 (1976).
R V Taylor, W Scott, P R Findley, Z Wu, W C Walker and K M Monaghan, *J Chem Phys*, 74, 3718, (1981).
W C Walker, R V Taylor and K M Monahan, *Chem Phys Lett*, 84, 288, (1981).